# Excitation–Contraction Coupling of the Mouse Embryonic Cardiomyocyte

Risto Rapila, Topi Korhonen, and Pasi Tavi

Institute of Biomedicine, Department of Physiology and Biocenter Oulu, University of Oulu, 90014 Oulu, Finland

In the mammalian embryo, the primitive tubular heart starts beating during the first trimester of gestation. These early heartbeats originate from calcium-induced contractions of the developing heart muscle cells. To explain the initiation of this activity, two ideas have been presented. One hypothesis supports the role of spontaneously activated voltage-gated calcium channels, whereas the other emphasizes the role of $Ca^{2+}$ release from intracellular stores initiating spontaneous intracellular calcium oscillations. We show with experiments that both of these mechanisms coexist and operate in mouse cardiomyocytes during embryonic days 9–11. Further, we characterize how inositol-3-phosphate receptors regulate the frequency of the sarcoplasmic reticulum calcium oscillations and thus the heartbeats. This study provides a novel view of the regulation of embryonic cardiomyocyte activity, explaining the functional versatility of developing cardiomyocytes and the origin and regulation of the embryonic heartbeat.

The Journal of General Physiology

## INTRODUCTION

Adult ventricular cardiomyocytes are not spontaneously active on their own, but instead are specialized to form an electrically excitable meshwork, where excitation relies on highly developed cell-to-cell contacts and specialized pacemaker cells. Compared with adult myocytes, embryonic cardiomyocytes show remarkable functional plasticity. They must be able to maintain their activity during transition periods without physical connections to other cells, enabling cell migration in the developing heart (Buckingham et al., 2005). In addition, these cardiomyocytes have the ability to synchronize their electrical activity and contraction with other cells to form coordinated contraction (Kamino, 1991), just like adult cardiomyocytes. This functional versatility of embryonic cardiomyocytes is essential to ensure the continuous beating of the heart muscle cells, a prerequisite for the survival of the embryo and development of the heart itself (Copp, 1995; Puceat and Jaconi, 2005).

The mechanisms behind the induction and maintenance of the initial activity of the cardiomyocytes have not been identified, but two separate, seemingly contradictory mechanisms have been proposed on the basis of experiments with isolated cells and genetically manipulated animals and cells. One line of evidence suggests that upon spontaneous depolarization of membrane voltage ($V_m$), calcium influx through voltage-activated calcium channels (VACCs) triggers myocyte contraction, with little or no contribution of calcium release from intracellular stores inside the SR (Nakanishi et al., 1988; Takeshima et al., 1998). Opposing data indicates that spontaneous SR calcium oscillations in fact drive the contractions and electrical activity (Viatchenko-Karpinski et al., 1999; Mery et al., 2005; Sasse et al., 2007). From the early stages of cardiogenesis, mammalian cardiomyocytes have both an excitable membrane with a variety of voltage-activated ion channels (Doevendans et al., 2000; Seisenberger et al., 2000; Cribbs et al., 2001) and a functional SR (Moorman et al., 2000; Seki et al., 2003), suggesting that the components for $V_m$ oscillation-driven calcium influx and SR-induced calcium release may coexist in the myocytes during early embryonic development. However, it is not known whether all embryonic cardiomyocytes possess both of these features or if specialized cell types are needed to fulfill these different tasks. We identify the mechanism by which spontaneous beating of solitary embryonic cardiomyocytes originates from oscillatory calcium releases from the SR. We further report that the same cells have a mechanism for action potential (AP)-induced calcium influx and subsequent CICR from the SR. These results explain the mechanisms of how the cardiac myocytes are autonomous in producing their basic activity during the early phases of heart development, yet are able to synchronize their activity with other myocytes. Further, we explain how these mechanisms are regulated to modify the beating rate of the developing heart. These characterized mechanisms could provide the explanation for

Correspondence to Pasi Tavi: pasi.tavi@oulu.fi

Abbreviations used in this paper: AM, acetoxymethyl; AP, action potential; E–C, excitation–contraction; $I_f$, hyperpolarization-activated current; $IP_3$, inositol-3-phosphate; $IP_3R$, $IP_3$ receptor; NCX, $NA^+/Ca^{2+}$ exchanger; RyR, ryanodine receptor; SL, sarcolemmal; VACC, voltage-activated calcium channel; $V_m$, membrane voltage.

The online version of this article contains supplemental material.



The Rockefeller University Press $30.00
J. Gen. Physiol. Vol. 132 No. 4 397–405
www.jgp.org/cgi/doi/10.1085/jgp.200809960

the origin and the regulation of the heartbeats before the differentiation of the functional pacemaker cells.

## MATERIALS AND METHODS

### Cell Isolation and Culturing

A previously described method was modified to isolate and culture embryonic days 9–11 (E9–11) embryonic cardiomyocytes (Sturm and Tam, 1993; Liu et al., 1999; Doevendans et al., 2000). Shortly, pregnant mice were killed by cervical dislocation. Embryos were excised and transferred to +2°C isolation buffer containing 100 mM NaCl, 10 mM KCl, 1.2 mM $KH_2PO_4$, 4 mM $MgSO_4$, 50 mM taurine, 20 mM glucose, and 10 mM HEPES (pH 6.9 with NaOH). Ventricles were cut from the embryos under a stereomicroscope. Dissected ventricles were incubated in the same solution containing 2 mg/ml pancreatin (Sigma-Aldrich) and 2 mg/ml collagenase type II (Worthington) for 50 min at 37°C on a rotating Ferris wheel. The tissue was mechanically dissociated by gentle trituration with a fire-polished glass pipette. The cell suspension was centrifuged at 750 *g* for 5 min followed by resuspension in Dulbecco's modified Eagle medium plus glutamax I (Invitrogen) with 10% FBS and 1% penicillin/streptomycin. Cells were plated on laminin-coated glass coverslips and incubated for 12–20 h at 37°C in a humidified 5% $CO_2$ incubator. Pregnant CD-1 mice from the Center for Experimental Animals at the University of Oulu were used. The experimental designs were approved by the Animal Use and Care Committee of the University of Oulu.

### Immunofluorescence Labeling and Microscopy

E10 cardiomyocytes were first cultured for 16 h on glass-bottom Petri dishes, and then rinsed with 0.1 M Tris-HCl, pH 7.3, fixed with 3% paraformaldehyde for 2 min, and permeabilized for 10 min with 0.5% Triton X-100. After washing with 0.1 M Tris-HCl, pH 7.3, twice for 5 min, the primary general ryanodine receptor (RyR; goat anti-RyR; Santa Cruz Biotechnology, Inc.) and general anti–inositol-3-phosphate ($IP_3$) receptor ($IP_3R$; rabbit anti-$IP_3R$ I/II/III; Santa Cruz Biotechnology, Inc.) antibodies were incubated for 1 h in 0.1 M Tris-HCl, pH 7.3, containing 10% FBS and 0.05% Triton X-100. Again, the specimens were washed twice and the secondary antibody (Alexa Fluor 488 chicken anti–goat and chicken anti–rabbit; Invitrogen) was incubated (pH 7.3) for 1 h. Dilutions for primary antibodies were 1:500, and the secondary antibody dilution was 1:750. After labeling, images were taken freshly with a confocal microscope (excitation 488 nm, emission 505–600, and 60× objective; FV1000; Olympus) at 0.2 µm/pixel spatial resolution.

### Confocal $Ca^{2+}$ Imaging

Primary isolated E9–11 embryonic cardiomyocytes were grown on laminin-coated glass-bottom Petri dishes for 12–20 h. Because cardiomyocytes are known to differentiate during long culture periods (Husse and Wussling, 1996; Zimmermann et al., 2002), the culturing times of the cells before starting the experiments were kept to a minimum. 12–20 h was considered sufficient time for the cells to recover from the isolation, but short enough to prevent them from further differentiating in culture. Cardiomyocytes were loaded with Fluo-4-acetoxymethyl (AM)-ester (1 µM dissolved in pluronic DMSO; Invitrogen) in culture medium for 30 min at 37°C in an incubator. The solution was changed twice, and cells were incubated at 37°C for at least 30 min for the dye to de-esterify. After this, the culturing dishes were placed in a custom-made perfusion system built into a confocal inverted microscope (FluoView 1000; Olympus). Cells were held at a steady 34°C by continuous superfusion with preheated Dulbecco's modified Eagle medium plus glutamax I (Invitrogen) culturing medium (pH 7.4, bubbled with 95% $O_2$/5% $CO_2$). To measure myocyte calcium signals, Fluo-4–loaded myocytes were excited at 488 nm and the emitted light was collected with a spectral detector from 520 to 620 nm through a 20× objective lens. To excite the cells, myocytes were stimulated with 1-ms voltage pulses 50% over the excitation threshold through two platinum wires located on both sides of the Petri dish. At the time of electrical stimulation or spontaneous activity, cells were line scanned at 400–600 Hz depending on the length of the scanning line, with a fixed pixel time of 10 µs. The frame scan images (256 × 256 pixels) were acquired at 23.7 Hz through a 20× objective and converted into a movie file (FluoView 1000; Olympus). The line scan images were analyzed with the ImageJ 1.36b (http://rsb.info.nih.gov/ij/) and Origin 7.5 (OriginLab Co.) programs. Fluo-4 fluorescence intensity is expressed as an $F/F_0$-ratio, where F is the background subtracted fluorescence intensity and $F_0$ is background subtracted minimum fluorescence value measured from each cell at rest.

### Electrophysiological Recordings

Primary isolated E9-11 embryonic cardiomyocytes were placed sparsely on laminin-coated glass-bottom Petri dishes and cultured for 12–20 h. The whole cell patch-clamp method was used to record whole cell currents and APs. Electrode resistances were 1–5 MΩ in whole cell current recordings and 10–15 MΩ in AP recordings. The membrane capacitances were measured by applying a 5-mV pulse to the holding potential. The hyperpolarization-activated current ($I_f$) was measured by applying voltage clamps ranging from −50 to −120 mV with 10-mV steps from a 0-mV holding potential. $I_f$ was defined as the difference between the initial current at the beginning of the voltage clamp and the current at the end of the voltage clamp. The solutions and the protocol were adopted from a previous report (Yasui et al., 2001). The external solution contained 137 mM NaCl, 5.4 mM KCl, 0.5 mM MgCl, 1 mM $CaCl_2$, 11.8 mM HEPES, 10 mM glucose, 2 mM $BaCl_2$, 2 mM $NiCl_2$, and 0.5 mM 4-AP, pH 7.40 (NaOH), and the pipette solution contained 80 mM KCl, 60 mM K-aspartic acid, 5 mM $Na_2$-phosphocreatine, 5 mM Mg-ATP, 0.65 mM $CaCl_2$, 10 mM EGTA, and 5 mM HEPES, pH 7.20 (KOH). APs were measured using the current clamp mode (I = 0). In some experiments when APs were recorded together with $[Ca^{2+}]_i$, cells were preloaded with Fluo-4 and the cells were continuously line-scanned (see above) at the time of $V_m$ recordings. The intracellular solution used was the same as described previously (Yang et al., 2005) and contained 120 mM K-aspartate, 25 mM KCl, 1 mM $MgCl_2$, 2 mM $Na_2$ phosphocreatine, 4 mM $Na_2ATP$, 2 mM NaGTP, 10 mM EGTA, and 5 mM HEPES, pH 7.2 (KOH), and the bath solution was Dulbecco's modified Eagle medium plus glutamax I (Invitrogen). The $Na^+/Ca^{2+}$ current ($I_{NCX}$) and $[Ca^{2+}]_i$ were recorded simultaneously using the $Ca^{2+}$ imaging methods and perforated-patch whole cell voltage clamp (120 µg/ml amphotericin-B). Solutions and protocol were as described previously (Ginsburg and Bers, 2005), except that the $V_m$ was clamped to −70 mV in $I_{NCX}$ recordings. To block $I_{NCX}$, 10 mM $Ni^{2+}$ was added. The bath solution contained 140 mM NaCl, 4 mM CsCl, 1 mM $MgCl_2$, 2 mM $CaCl_2$, and 10 mM HEPES, pH 7.4 (NaOH) plus 10 mM $NiCl_2$, and the pipette contained 40 mM CsCl, 80 mM Cs-methanesulfonate, 1 mM $MgCl_2$, 1 mM KCl, and 10 mM HEPES, pH 7.2 (CsOH). Whole cell currents were filtered at 2 kHz and acquired at 10 kHz. Clampex 9.2 software and Axopatch-1D amplifier and Digidata 1322A A/D-D/A (Axon Instruments) were used to control the command potentials and data acquisition. All electrophysiological measurements were done at +34°C. Data analysis was made using the Clampfit 9.2 (Axon Instruments), Origin 7.5 (OriginLab Corporation), and Matlab 6.5 (The Mathworks) software. Clampfit's leak resistance subtraction and software filters were used when necessary. The membrane currents were scaled by dividing them with the cell membrane capacitance.

### Statistics

Results are expressed as mean ± SEM. Statistical significance of difference was analyzed using the paired *t* test and one-way ANOVA. The $r^2$ and p-values for linear fit were determined using unweighted linear regression.

### Online Supplemental Material

The online supplemental material includes a video from a spontaneously active embryonic cardiomyocyte, which is loaded with Fluo-4 and frame scanned with a confocal microscope. Video 1 is available at http://www.jgp.org/cgi/content/full/jgp.200809960/DC1.

## RESULTS

### Origin of the Intracellular [$Ca^{2+}$] Oscillations

To elucidate the mechanisms triggering cardiomyocyte activity we did confocal $[Ca^{2+}]_i$ imaging and electrophysiological measurements from spontaneously beating isolated single embryonic (E9–11) myocytes. Without physical connections to other cells, isolated embryonic myocytes contract spontaneously at a rate of 0.40 ± 0.03 Hz ($n$ = 94), accompanied by oscillations in $[Ca^{2+}]_i$ and $V_m$ (Table I). It was suggested earlier that spontaneous plasmalemmal APs triggered by the $I_f$ initiate this activity (Nakanishi et al., 1988; Takeshima et al., 1998). If so, inhibition of this current should stop the spontaneous activity of these cells. Zeneca ZD7288 has been shown to be an efficient blocker of $I_f$ in adult guinea pig sinoatrial node cells (BoSmith et al., 1993), and we wanted to test if it could also be used to block the $I_f$ of the embryonic cardiomyocytes. Therefore, we measured $I_f$ with whole cell patch clamp from isolated E10 cardiomyocytes by applying voltage clamps ranging from −50 to −130 mV, with 10-mV steps from a 0-mV holding potential as described previously (Yasui et al., 2001). In these conditions, Zeneca was found to be a very effective blocker of embryonic $I_f$. 10 µM Zeneca reduced $I_f$ by ∼86% (Fig. 1 A), from −2.50 ± 0.26 pA/pF to −0.35 ± 0.40 pA/pF (at −130 mV; P = 0.002; $n$ = 7). When 10 µM Zeneca was applied to spontaneously active E9–11 cardiomyocytes, the frequency of the spontaneous oscillations was slightly reduced in four out of seven myocytes and no change was observed in three out of seven. Because this effect was not consistent, the effect of $I_f$ block on the frequency or the amplitude of the spontaneous calcium signals was not statistically significant (Fig. 1, B–D). We next asked if the suggested spontaneous SR calcium oscillations (Sasse et al., 2007) could provide an alternative explanation for this activity. Therefore, we did confocal calcium imaging of the E9–11 cardiomyocytes to characterize the spatio-temporal properties of the spontaneous calcium signals. We noticed that calcium signals are initiated at the vicinity of the thin perinuclear area (Fig. 2 A) corresponding to the location of the SR in developing cardiomyocytes (Mesaeli et al., 1999). After the initial release from the SR, calcium diffuses in the cytosol and the $[Ca^{2+}]_i$ increases near the plasma membrane after a delay (Fig. 2 A and Video 1, which is available at http://www.jgp.org/cgi/content/full/jgp.200809960/DC1). The delay between $[Ca^{2+}]_i$ rise near the SR and near the sarcolemmal (SL) varied from 8 to 68 ms, with 28.5 ± 4.9 ms ($n$ = 12) average delay. This SR calcium release appeared to be relatively well developed; the amplitude of the spontaneous global calcium signal was 56.5 ± 0.5% ($n$ = 23) of the amplitude of the caffeine-induced calcium transient, indicating that 56.5% of the available

TABLE I

*Characteristics of Embryonic Cardiomyocyte Calcium Signals and APs*

| *Parameter (unit)* | *Value (mean ± SEM)* | ***n*** |
|---|---|---|
| Frequency of activity (Hz) | 0.40 ± 0.03 | 94 |
| $[Ca^{2+}]$ transient amplitude (Fluo-4, $F/F_0$) | 0.90 ± 0.05 | 94 |
| Decay (τ) of the $[Ca^{2+}]$ transient (ms) | 1,191 ± 95 | 94 |
| r.p. (mV) | −57.2 ± 0.9 | 27 |
| $dV/dt_{max}$ (mV/ms) | 77.9 ± 19.7 | 27 |
| AP amplitude (mV) | 95.6 ± 2.7 | 27 |
| $APD_{90}$ (ms) | 253.5 ± 27.5 | 27 |
| Maximum hyperpolarization after AP (mV) | 11.1 ± 1.1 | 27 |

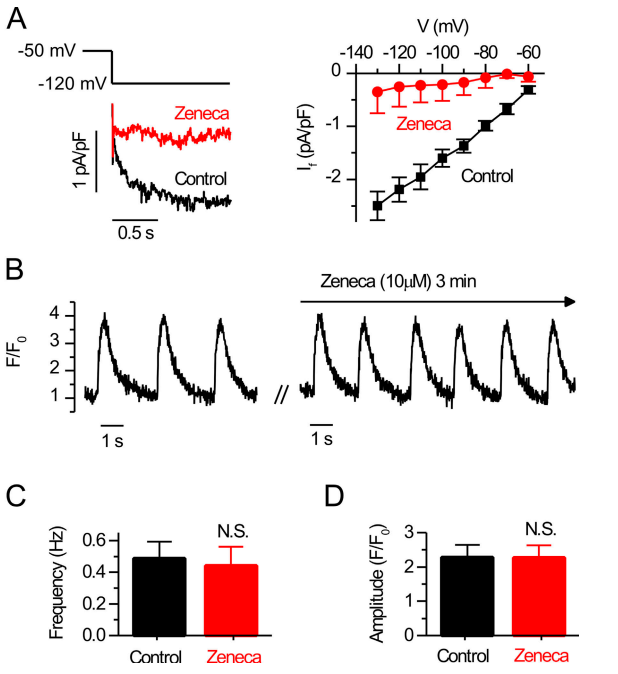


**Figure 1.** Inhibition of pacemaker ($I_f$) current does not inhibit spontaneous calcium signals of embryonic cardiomyocytes. (A) Representative recording showing the effect of 10 µM Zeneca on the $I_f$ (bottom left) elicted by hyperpolarization of the embryonic cardiomyocyte membrane from −50 to −120 mV in whole cell voltage clamp (top left) and the current–voltage relationship of the $I_f$ current with and without Zeneca (right). (B) Spontaneous calcium signals recorded from E10 cardiomyocytes before (left) and after application of the pacemaker current inhibitor Zeneca ZD7288 (right), and the effect on the frequency (C) and amplitude (D) of the calcium signals.

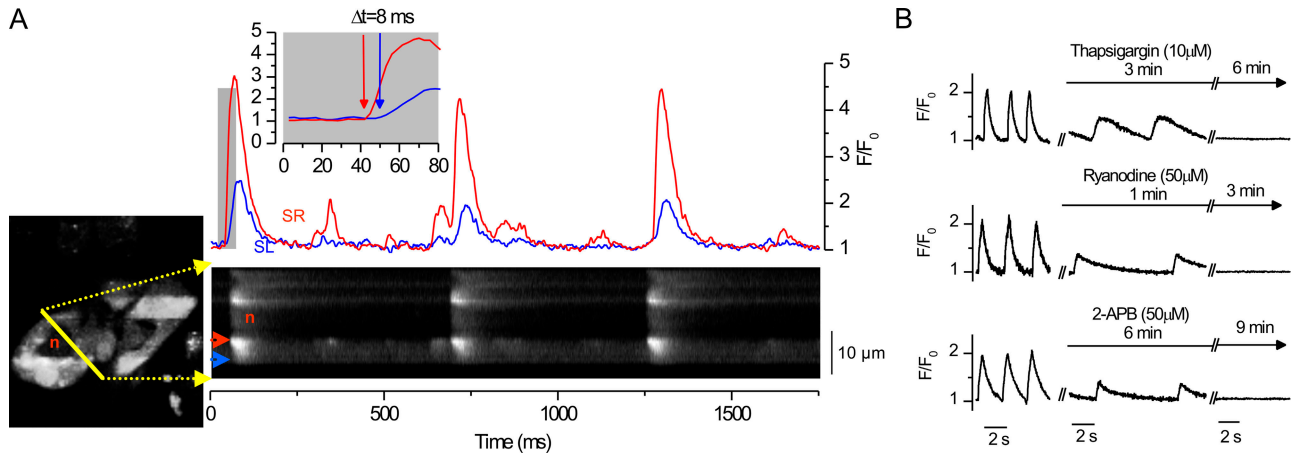


**Figure 2.** Spontaneous calcium release initiates cytosolic calcium oscillations in embryonic cardiac myocytes. (A) Laser scanning confocal image from a Fluo-4–loaded, isolated E10 spontaneously active cardiomyocyte (left) with corresponding line scan (yellow line) through the cytosol surrounding the dark nuclear area (red n). Red and blue arrowheads in the line scan image denote near SR area and near SL area, respectively. Graphs above the line scan image show relative calcium signals (Fluo-4 emission, $F/F_0$) from near SR (red line) and near SL (blue line). Insert (gray background) shows both graphs in an expanded timescale from selected area below (gray). (B) Effects of inhibitors of SR $Ca^{2+}$-ATPase (10 µM thapsigargin; top), RyRs (50 µM ryanodine; middle), and $IP_3$Rs (50 µM 2-APB; bottom) on spontaneous calcium signals from isolated E10 cardiomyocytes.

SR calcium is released during each spontaneous calcium release. To occur, SR calcium release seems to require intact calcium uptake as well as two types of SR calcium release channels because blocking either $IP_3$Rs (with 2-APB) (Maruyama et al., 1997) ($n = 14$) or RyRs (with ryanodine; $n = 27$), as well as inhibiting SR calcium uptake (with thapsigargin; $n = 11$), initially slows down the spontaneous activity until the cells show no calcium signals (Fig. 2 B).

## Regulation of the Rate of the Spontaneous SR $Ca^{2+}$ Oscillations

It seems that both types of SR calcium release channels (RyRs and $IP_3$Rs) are needed for spontaneous calcium

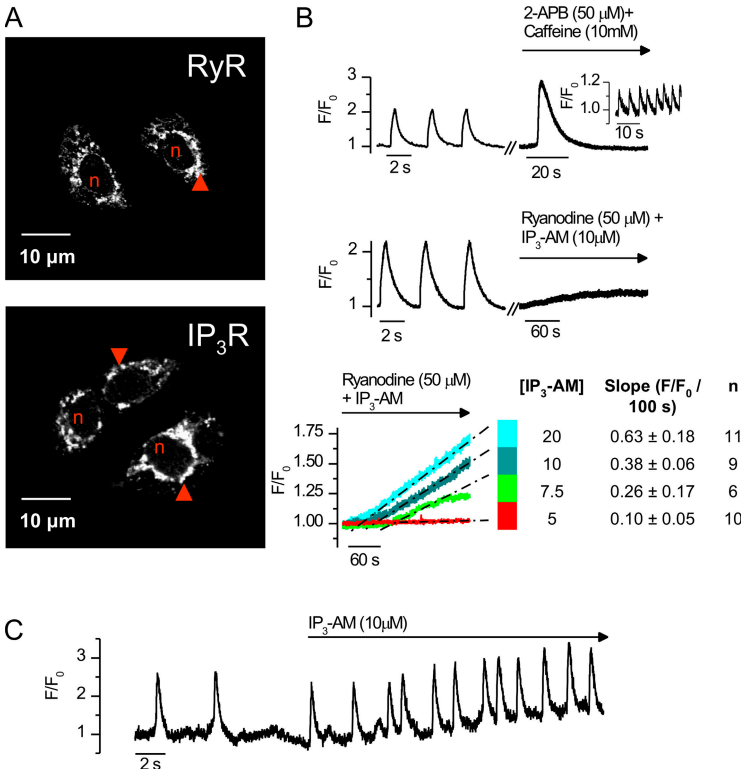


**Figure 3.** $IP_3$Rs regulate the frequency of the spontaneous SR calcium releases. (A) RyR (top) and $IP_3$R (bottom) immunolabeling in isolated E10 embryonic cardiomyocytes. Red arrowheads indicate specific staining pattern around nuclei (red n). (B) When $IP_3$Rs are inhibited with 2-APB, rapid application of 10 mM caffeine activates RyRs to release calcium ($n = 10$), and slower application of caffeine ($n = 5$) induces frequent oscillatory calcium releases (insert). In an identical experimental arrangement, when RyRs are inhibited with 50 µM ryanodine and $IP_3$Rs are stimulated with $IP_3$AM, a sustained calcium leak is triggered that is proportional to the applied [$IP_3$AM] (bottom). (C) Application of membrane-permeable $IP_3$ ($IP_3$-AM) increases the frequency of spontaneous calcium oscillations in isolated E10 cardiac myocytes.

signals, but what are the specific roles of the different channel types? These different types of $Ca^{2+}$ release channels, RyRs and $IP_3$Rs, are located perinuclearly, presumably on the thin SR around the nucleus (Fig. 3 A). Both channel types act as functional calcium release channels in E10 myocytes because pharmacological activation of RyRs alone produces robust calcium release ($n = 10$) or frequent repetitive calcium oscillations ($n = 5$), and stimulation of $IP_3$Rs with membrane-permeable $IP_3$AM (Li et al., 1997) at normal cellular $[Ca^{2+}]_i$ produces a constant SR calcium leak (Fig. 3 B). When cardiomyocytes were exposed to varying concentrations of $IP_3$AM (from 5 to 20 µM) and RyRs were blocked, the slope of the cytosolic calcium rise was increased in an $IP_3$AM concentration–dependent manner (Fig. 3 B), but oscillatory calcium signals were not observed even at the highest $IP_3$AM concentration. These results suggest a mechanism by which $IP_3$Rs provide the calcium leak that increases the cytosolic $[Ca^{2+}]_i$ and thereby increases the opening probability of the RyRs, promoting the spontaneous $Ca^{2+}$ releases. If so, increase of the $IP_3$-dependent leak should result in more frequent calcium releases when the RyRs are not blocked. To demonstrate this, we exposed E10 cardiomyocytes to 10 µM of membrane-permeable $IP_3$ and noticed that the spontaneous rate of calcium release events and consequently the beating frequency in myocyte cultures increased by 27.3 ± 9.2% ($n = 7$; $P < 0.05$; Fig. 3 C).

### The Mechanisms for Plasmalemmal Electrical Activity

Embryonic myocytes have several depolarizing currents, including a sodium current (Doevendans et al., 2000), T- and L-type calcium currents (Seisenberger et al., 2000; Cribbs et al., 2001), and a pacemaker current ($I_f$) (Yasui et al., 2001) that together constitute an electrically excitable membrane, which might in theory generate spontaneous $V_m$ oscillations and pacemaker-type APs (Yasui et al., 2001). However, because embryonic myocytes also have a prominent $Na^+/Ca^{2+}$ exchanger (NCX) current (Shepherd et al., 2007), it was suggested (Janowski et al., 2006; Sasse et al., 2007) that the spontaneous SR calcium release might induce a depolarizing current by activating the NCX and thereby trigger APs. Several independent original findings of the present study support this latter idea. First, we found that inhibition of $I_f$ by 10 µM Zeneca has no significant effect on the frequency or amplitude of the spontaneous calcium oscillations (Fig. 1, C and D) or accompanying $V_m$ parameters,

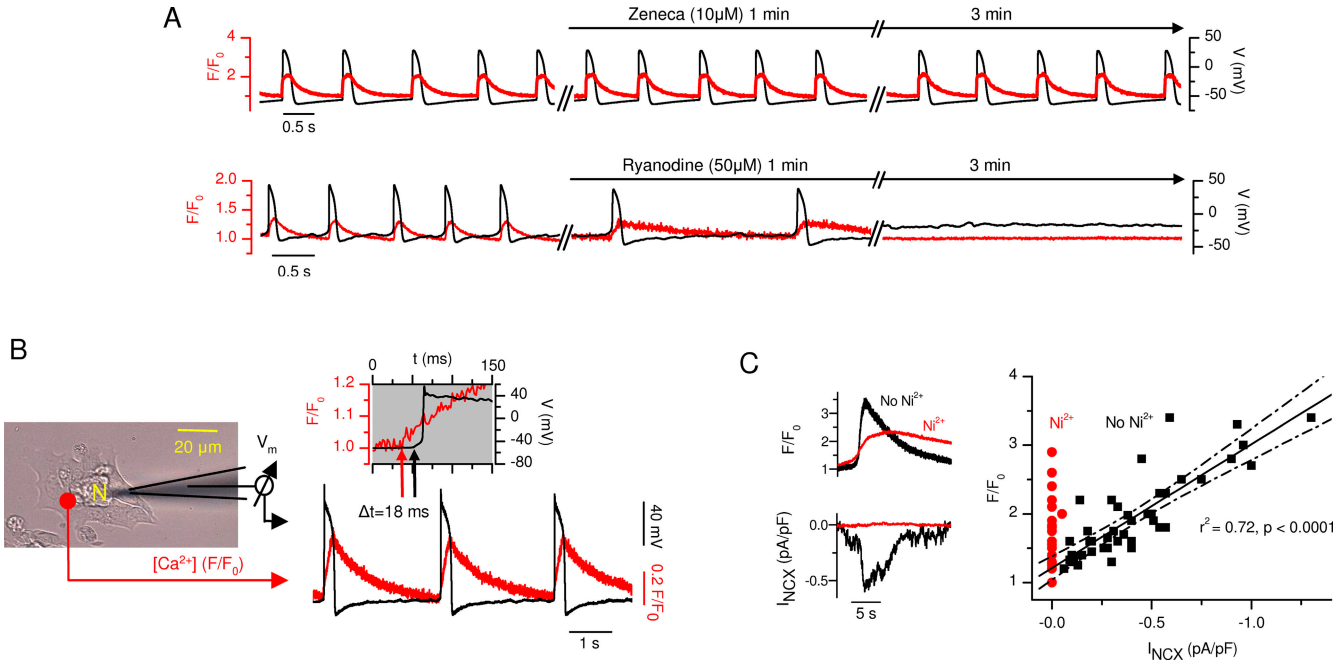


**Figure 4.** APs are triggered by spontaneous calcium oscillations. (A) Representative traces from simultaneous $V_m$ and $[Ca^{2+}]_i$ measurements during $I_f$ inhibition by Zeneca ($n = 6$; top) and SR inhibition by ryanodine ($n = 5$; bottom) from an E10 cardiomyocyte, demonstrating that inhibition of SR calcium release blocks the generation of APs, whereas inhibition of $I_f$ does not. (B) Simultaneous $V_m$ and $[Ca^{2+}]_i$ measurements from a spontaneously active E10-isolated cardiomyocyte showing the time difference between SR calcium release (location indicated in the phase contrast image with a red dot) and AP upstroke. The insert (gray background) shows both graphs in an expanded timescale with an 18-ms delay between the beginning of the release and initiation of AP upstroke. (C) Caffeine-induced calcium release (top) with corresponding inward current (bottom) in the absence and presence of 10 mM $Ni^{2+}$, a blocker of the NCX. Right-side graph shows the relationship between cytosolic calcium and NCX current density at variable $[Ca^{2+}]_i$ levels pooled from 22 measurements during caffeine-induced calcium releases. Linear regression fit (solid line) with 95% confidence bands (dotted lines) shows a strong correlation between $F/F_0$ and NCX current density with a regression coefficient ($r^2$) of 0.72 ($P < 0.0001$). In the presence of $Ni^{2+}$, calcium signals fail to trigger an inward current (red dots).

namely resting potential, AP amplitude, or AP duration at 90% repolarization ($n$ = 6), whereas suppression of the SR calcium release inhibits the APs ($n$ = 5; Fig. 4 A). Second, our measurements showed that calcium release at the surface of the SR precedes the $V_m$ depolarization with a delay that is in accordance with the time necessary for the calcium diffusion through the cytosol (Fig. 4 B). Third, after each SR calcium release event an inward current was triggered. This current was proportional to $[Ca^{2+}]_i$ and was sensitive to $Ni^{2+}$ (Fig. 4 C), indicating that the current was induced by $Na^+$ influx during calcium removal by the electrogenic NCX.

### The Role of Plasmalemmal $Ca^{2+}$ Fluxes in SR Calcium Oscillations

Intuitively, without subsequent compensatory Ca influx, calcium extrusion by the NCX during the initiation of each AP would gradually deplete the calcium stores. Therefore, it would be natural to assume that during SR-driven spontaneous activity, the plasmalemmal voltage–activated calcium influx could provide this compensatory calcium influx. Supporting this idea, blocking the L-type calcium channel suppressed spontaneous calcium signals and eventually inhibited calcium release and AP generation (Fig. 5 A). However, this effect is not due to the direct impact of the L-type channel block, but rather caused by simultaneous ~60% ($P < 0.001$; $n$ = 8) depletion of SR calcium (Fig. 5 B). This suggests that voltage-activated calcium influx compensates for the NCX-mediated $Ca^{2+}$ extrusion, maintaining the SR calcium stores and thus securing the SR capacity to produce oscillatory calcium releases. If this was true, blocking the L-type channel current and the NCX current simultaneously would leave SR calcium oscillations intact. Supporting this idea, when we applied nifedipine to inhibit the L-type current together with $Ni^{2+}$ to block the NCX current, the cells were able to maintain SR calcium oscillation significantly longer than with nifedipine alone (Fig. 5 C). This suggests that in the absence of calcium fluxes through the plasmalemma, the SR calcium oscillations might continue independently.

### Role of CICR

It was previously suggested that in mouse embryonic cardiomyocytes (E9.5), RyR channels serve as SR leak channels rather than being activated by incoming calcium through VACCs during AP to promote CICR (Takeshima et al., 1998). To test this, we exposed E9–11 cardiomyocytes to electrical pacing, which would reveal if stimulated APs could synchronize the calcium signals by recruiting VACCs to trigger CICR via RyRs. We noticed that the SR-driven activity was indeed synchronized by stimulated

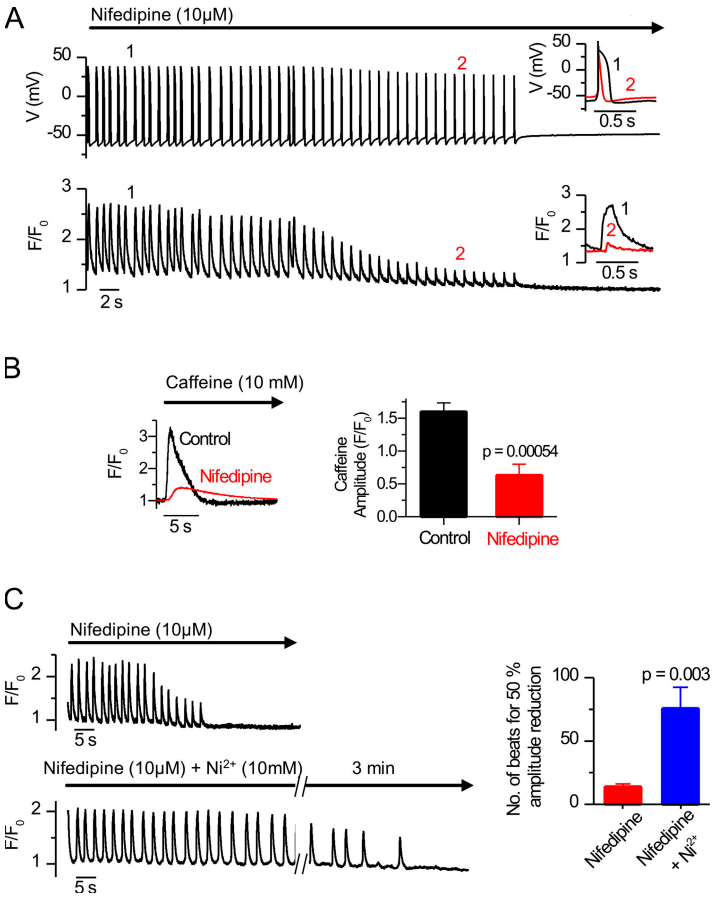


**Figure 5.** Plasmalemmal calcium influx is needed to maintain the SR calcium stores when calcium is extruded by the NCX. (A) L-type calcium channel inhibitor nifedipine (10 μM) suppresses spontaneous calcium signals (bottom left), modulates the shape of APs, and eventually inhibits AP generation. (B) This is accompanied by simultaneous depletion of SR calcium content as estimated by rapid application of caffeine ($n$ = 24 control plus 8 nifedipine). (C) When the NCX is blocked (with $Ni^{2+}$) together with inhibition of L-type calcium channels (with nifedipine; bottom left), embryonic cardiomyocytes retain their spontaneous activity longer compared with the application of nifedipine alone (top left). This is measured as the number of spontaneous oscillations before the calcium-transient amplitude is reduced to 50% of its original value (right).

APs (Fig. 6 A) and, in fact, 67.5 ± 2.3% ($n$ = 23) of the amplitude of the AP-induced calcium transient originated from CICR (Fig. 6 B). This suggests that the same cells are capable of producing spontaneous activity and synchronize their activity upon sufficient electrical stimulation.

## DISCUSSION

Here, we present experimental data elucidating the regulation of the embryonic cardiomyocyte $[Ca^{2+}]_i$ signals and $V_m$. We show that spontaneous activity of the solitary cardiomyocytes at E9–11 is triggered by calcium release from the SR upon activation of both RyRs and $IP_3Rs$ (Figs. 2 and 3). The resulting $[Ca^{2+}]_i$ signals are sufficient for activating contraction as well as for triggering APs via the NCX current (Fig. 4). In addition, the same cells are capable of generating APs and calcium influx and concomitantly trigger CICR from the SR upon sufficient electrical excitation (Fig. 6). At E9–11, these features seem to be common to all cardiomyocytes tested. According to our results, the primary activity of the developing cardiomyocytes relies on the SR calcium oscillations. However, at the same time, myocytes have an excitable membrane and external electrical stimulation can trigger an AP and subsequent voltage-activated $Ca^{2+}$ intrusion and CICR. By this mechanism, APs are conducted from cell to cell and contraction of adjacent cells is synchronized to generate a heartbeat. We also describe how the factors that modulate SR calcium release will also affect the beating rate of the cardiomyocytes and therefore the output of the developing heart (Fig. 3).

### The Role of SR Calcium Oscillations in Embryonic Pacemaking

This study and others (Viatchenko-Karpinski et al., 1999; Mery et al., 2005; Sasse et al., 2007) have shown that an intact SR is required for the spontaneous embryonic heartbeats. In addition, intact SR is required for normal heart development because mice deficient in the major embryonic calcium buffer located in the SR, calreticulin, show embryonic malformations, impaired calcium signaling, and compromised calcium-dependent transcription (Mesaeli et al., 1999). We showed that blocking of any of the SR $Ca^{2+}$ release channels, $IP_3R$ or RyR, or the SR $Ca^{2+}$ pump SERCA diminished and finally stopped the $Ca^{2+}$ signals and APs (Fig. 2 B). We found that stimulation of $IP_3R$ only increased SR $Ca^{2+}$ leak but did not induce global cytosolic $[Ca^{2+}]_i$ transients, and that for global spontaneous cytosolic $[Ca^{2+}]_i$ transients, RyR activation was a prerequisite (Fig. 3). Accordingly, mice deficient in the cardiac isoform of the RyR (RyR-2) have impaired calcium signals, and the development of SR and mitochondria are consequently disturbed (Takeshima et al., 1998). However, genetic ablation of any of the individual $IP_3R$ subtypes alone does not produce any evident cardiac phenotype in mouse. Lack of $IP_3R$ type 1 results in the most dramatic phenotype, with increased embryonic lethality and severe neurological malformations (Matsumoto et al., 1996). Both $IP_3R$ type 2 and 3 knockout mice are viable and have no obvious defects, whereas double knockout ($IP_3R2^{-/-}$ plus $IP_3R3^{-/-}$) mice die within 4 wk after birth due to defects in the intracellular calcium handling of endocrine cells and consequent metabolic disturbances (Futatsugi et al., 2005). This suggests that none of the $IP_3R$ types is indispensable in heart development, but it does not rule out the possibility that total lack of $IP_3R$ activity might induce more drastic changes. In embryonic stem cell–derived cardiomyocytes, $IP_3R$ antisense against the predominant $IP_3R$ isoform in these cells, as well as pharmacological inhibition of $IP_3R$ activity, abolishes the spontaneous activity of the cells (Mery et al., 2005), just as in this study (Fig. 2 B). In theory, RyRs are capable of producing oscillatory $Ca^{2+}$ releases on their own, but the frequency of these oscillations would be an order of magnitude slower than what we observed in E9–11 cardiomyocytes (Keizer and Levine, 1996). We found that increases in the spontaneous RyR openings are dependent on the $Ca^{2+}$ leak via $IP_3R$ (Fig. 3 C), which stimulates the RyRs to open and subsequently increases the frequency of the global $[Ca^{2+}]_i$ transients in E9–11 cardiomyocytes. This study illuminates how the interaction between multiple factors modulating cytosolic $[IP_3]$ levels will also regulate the embryonic heart rate.

Recently, it was shown that in some of the early embryonic cardiomyocytes, the activity originates from local high frequency (~4 Hz) $Ca^{2+}$ oscillations (Sasse et al., 2007). Similar calcium signals were also seen in this study (Fig. 2 A), suggesting that SR also produces "subthreshold" calcium events, spark-like local signals that are not large enough to propagate over the whole SR surface and recruit the majority of the $Ca^{2+}$-release units. However, it is not clear whether these signals serve a true physiological function in triggering force-producing contractions or if they only represent the noise of the system.

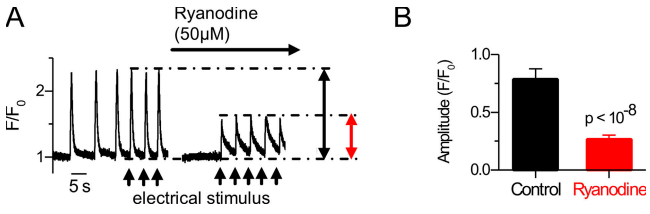


**Figure 6.** Embryonic cardiomyocytes have prominent CICR. (A) A spontaneously active isolated E10 cardiomyocyte produces electrically stimulated calcium transients (black arrowheads). (B) The amplitude of the electrically induced calcium transients was significantly suppressed by ryanodine (right; $n$ = 23).

According to our results, isolated embryonic cardiomyocytes have a lower spontaneous beating rate (~0.4 Hz) than the developing heart in utero (~2 Hz; Gui et al., 1996). This might be due to the fact that in the intact embryonic heart in utero, the myocytes are subjected to a variety of diffuse hormonal and local hormonal stimuli, which modify the cellular components involved in the pacemaking of the cells and are not present in embryonic cardiomyocyte cultures. In addition to the known stimulatory effects of several hormones and neurotransmitters on the embryonic heartbeat, such as catecholamines (Ebert and Taylor, 2006), we actually report an $IP_3$-dependent mechanism that speeds up the embryonic heart rate (Fig. 3 C), suggesting that all of the hormones able to regulate $IP_3$ production (e.g., AngII, ET-1, and α-adenergic stimuli) also affect the heart rate. In addition, it is likely that the heart rate of the intact heart is defined by the myocyte with the highest frequency of spontaneous activity. Therefore, the average frequencies of the isolated myocytes and the frequency of the intact heart are not strictly comparable.

### Interplay between SL Ion Currents and SR Calcium Release

Most of the recent knowledge of embryonic excitation–contraction (E–C) coupling originates from studies with genetically engineered mouse models, which collectively suggest that several components are involved in the regulation of the embryonic heartbeat. So far, genetic deletion or suppression of any of the key components of E–C coupling has produced phenotypes with severe heart malformations and functional impairments that induce early embryonic lethality. Knockout of the *HCH4* gene, coding the pacemaker current $I_f$ channel, slows down the heart rate at E9.5 and abolishes the formation of mature pacemaker cells (Stieber et al., 2003). Similarly, genetic suppression of L-type calcium channels slows down the heart rate at E10.5, but it also reduces the cytosolic calcium signals (Weissgerber et al., 2005). Both adult and embryonic cardiomyocytes express the electrogenic plasmalemmal $Na^+$-$Ca^{2+}$ exchanger (NCX) for calcium extrusion (Koban et al., 1998). Targeted inactivation of cardiac NCX leads to embryonic lethality before E11, and the hearts of NCX-deficient ($NCX^{-/-}$) mice lack spontaneous heartbeats and organized contractile myofibrils (Koushik et al., 2001).

Our results suggest that in embryonic cardiomyocytes, two different mechanisms (SR- and AP-driven) can be separately recruited to generate global calcium signals (Figs. 2 and 6). During SR calcium oscillations, when the NCX extrudes calcium and triggers APs, SL calcium influx is required to maintain SR calcium content and secure global spontaneous $[Ca^{2+}]_i$ oscillations (Fig. 5 A). However, if $[Ca^{2+}]_i$ signals and $V_m$ are uncoupled by blocking the NCX, the SR calcium oscillations can be produced independently of the SL calcium fluxes (Fig. 5 C). Similarly, the generation of AP-induced calcium signals can be dissected into two separate parts. Upon generation of electrically evoked APs, embryonic cardiomyocytes produce $[Ca^{2+}]_i$ signals that are mainly based on SR calcium release (CICR) (Fig. 6). However, in the absence of SR calcium release, myocytes are still able to produce global whole cell $[Ca^{2+}]_i$ signals based only on voltage-activated SL calcium intrusion (Fig. 6).

Coexistence of the pacemaking and E–C coupling mechanism in the same cells explains how embryonic cardiomyocytes maintain their activity during transition periods without physical connections to other cells, enabling cell migration in the developing heart (Buckingham et al., 2005), and also how they are able to synchronize their electrical activity and contraction with other cells to form coordinated contraction (Kamino, 1991) of the heart. This study provides a novel view of the regulation of embryonic cardiomyocyte activity, characterizing the functional versatility of developing cardiomyocytes and further explaining fundamental phenomena in the origin of the heartbeat. In addition, although these results open interesting perspectives in the field of mammalian cardiac development, they also elucidate mechanisms that may be exploited in the development of cellular excitability and calcium signaling in general.

We thank S.L. Hänninen for valuable comments on the manuscript and A. Rautio for technical assistance.

This study was supported by the Finnish Heart Research Foundation, Academy of Finland, and Sigrid Juselius Foundation.

Olaf S. Andersen served as editor.

Submitted: 11 January 2008
Accepted: 19 August 2008

## REFERENCES

BoSmith, R.E., I. Briggs, and N.C. Sturgess. 1993. Inhibitory actions of ZENECA ZD7288 on whole-cell hyperpolarization activated inward current ($I_f$) in guinea-pig dissociated sinoatrial node cells. *Br. J. Pharmacol.* 110:343–349.

Buckingham, M., S. Meilhac, and S. Zaffran. 2005. Building the mammalian heart from two sources of myocardial cells. *Nat. Rev. Genet.* 6:826–835.

Copp, A.J. 1995. Death before birth: clues from gene knockouts and mutations. *Trends Genet.* 11:87–93.

Cribbs, L.L., B.L. Martin, E.A. Schroder, B.B. Keller, B.P. Delisle, and J. Satin. 2001. Identification of the T-type calcium channel (Ca(V)3.1d) in developing mouse heart. *Circ. Res.* 88:403–407.

Doevendans, P.A., S.W. Kubalak, R.H. An, K.D. Becker, K.R. Chien, and R.S. Kass. 2000. Differentiation of cardiomyocytes in floating embryoid bodies is comparable to fetal cardiomyocytes. *J. Mol. Cell. Cardiol.* 32:839–851.

Ebert, S.N., and D.G. Taylor. 2006. Catecholamines and development of cardiac pacemaking: an intrinsically intimate relationship. *Cardiovasc. Res.* 72:364–374.

Futatsugi, A., T. Nakamura, M.K. Yamada, E. Ebisui, K. Nakamura, K. Uchida, T. Kitaguchi, H. Takahashi-Iwanaga, T. Noda, J. Aruga, and K. Mikoshiba. 2005. $IP_3$ receptor types 2 and 3 mediate exocrine secretion underlying energy metabolism. *Science.* 309:2232–2234.

Ginsburg, K.S., and D.M. Bers. 2005. Isoproterenol does not enhance Ca-dependent Na/Ca exchange current in intact rabbit ventricular myocytes. *J. Mol. Cell. Cardiol.* 39:972–981.

Gui, Y.H., K.K. Linask, P. Khowsathit, and J.C. Huhta. 1996. Doppler echocardiography of normal and abnormal embryonic mouse heart. *Pediatr. Res.* 40:633–642.

Husse, B., and M. Wussling. 1996. Developmental changes of calcium transients and contractility during the cultivation of rat neonatal cardiomyocytes. *Mol. Cell. Biochem.* 164:13–21.

Janowski, E., L. Cleemann, P. Sasse, and M. Morad. 2006. Diversity of $Ca^{2+}$ signaling in developing cardiac cells. *Ann. NY Acad. Sci.* 1080:154–164.

Kamino, K. 1991. Optical approaches to ontogeny of electrical-activity and related functional-organization during early heart development. *Physiol. Rev.* 71:53–91.

Keizer, J., and L. Levine. 1996. Ryanodine receptor adaptation and $Ca^{2+}$-induced $Ca^{2+}$ release-dependent $Ca^{2+}$ oscillations. *Biophys. J.* 71:3477–3487.

Koban, M.U., A.F.M. Moorman, J. Holtz, M.H. Yacoub, and K.R. Boheler. 1998. Expressional analysis of the cardiac Na-Ca exchanger in rat development and senescence. *Cardiovasc. Res.* 37:405–423.

Koushik, S.V., J. Wang, R. Rogers, D. Moskophidis, N.A. Lambert, T.L. Creazzo, and S.J. Conway. 2001. Targeted inactivation of the sodium-calcium exchanger (Ncx1) results in the lack of a heartbeat and abnormal myofibrillar organization. *FASEB J.* 15:1209–1211.

Li, W.H., C. Schultz, J. Llopis, and R.Y. Tsien. 1997. Membrane-permeant esters of inositol polyphosphates, chemical syntheses and biological applications. *Tetrahedron.* 53:12017–12040.

Liu, W., K. Yasui, A. Arai, K. Kamiya, J. Cheng, I. Kodama, and J. Toyama. 1999. beta-adrenergic modulation of L-type $Ca^{2+}$-channel currents in early-stage embryonic mouse heart. *Am. J. Physiol.* 276:H608–H613.

Maruyama, T., T. Kanaji, S. Nakade, T. Kanno, and K. Mikoshiba. 1997. 2APB, 2-aminoethoxydiphenyl borate, a membrane-penetrable modulator of Ins(1,4,5)$P_3$-induced $Ca^{2+}$ release. *J. Biochem. (Tokyo).* 122:498–505.

Matsumoto, M., T. Nakagawa, T. Inoue, E. Nagata, K. Tanaka, H. Takano, O. Minowa, J. Kuno, S. Sakakibara, M. Yamada, et al. 1996. Ataxia and epileptic seizures in mice lacking type 1 inositol 1,4,5-trisphosphate receptor. *Nature.* 379:168–171.

Mery, A., F. Aimond, C. Menard, K. Mikoshiba, M. Michalak, and M. Puceat. 2005. Initiation of embryonic cardiac pacemaker activity by inositol 1,4,5-trisphosphate-dependent calcium signaling. *Mol. Biol. Cell.* 16:2414–2423.

Mesaeli, N., K. Nakamura, E. Zvaritch, P. Dickie, E. Dziak, K.H. Krause, M. Opas, D.H. MacLennan, and M. Michalak. 1999. Calreticulin is essential for cardiac development. *J. Cell Biol.* 144:857–868.

Moorman, A.F.M., C.A. Schumacher, P.A.J. de Boer, J. Hagoort, K. Bezstarosti, M.J.B. van den Hoff, G.T.M. Wagenaar, J.M.J. Lamers, F. Wuytack, V.M. Christoffels, and J.W.T. Fiolet. 2000. Presence of functional sarcoplasmic reticulum in the developing heart and its confinement to chamber myocardium. *Dev. Biol.* 223:279–290.

Nakanishi, T., M. Seguchi, and A. Takao. 1988. Development of the myocardial contractile system. *Experientia.* 44:936–944.

Puceat, M., and M. Jaconi. 2005. $Ca^{2+}$ signalling in cardiogenesis. *Cell Calcium.* 38:383–389.

Sasse, P., J. Zhang, L. Cleemann, M. Morad, J. Hescheler, and B.K. Fleischmann. 2007. Intracellular $Ca^{2+}$ oscillations, a potential pacemaking mechanism in early embryonic heart cells. *J. Gen. Physiol.* 130:133–144.

Seisenberger, C., V. Specht, A. Welling, J. Platzer, A. Pfeifer, S. Kuhbandner, J. Striessnig, N. Klugbauer, R. Feil, and F. Hofmann. 2000. Functional embryonic cardiomyocytes after disruption of the L-type alpha(1C) (Ca(v)1.2) calcium channel gene in the mouse. *J. Biol. Chem.* 275:39193–39199.

Seki, S., M. Nagashima, Y. Yamada, M. Tsutsuura, T. Kobayashi, A. Namiki, and N. Tohse. 2003. Fetal and postnatal development of $Ca^{2+}$ transients and $Ca^{2+}$ sparks in rat cardiomyocytes. *Cardiovasc. Res.* 58:535–548.

Shepherd, N., V. Graham, B. Trevedi, and T. Creazzo. 2007. Changes in regulation of sodium/calcium exchanger of avian ventricular heart cells during embryonic development. *Am. J. Physiol. Cell Physiol.* 292:C1942–C1950.

Stieber, J., S. Herrmann, S. Feil, J. Loster, R. Feil, M. Biel, F. Hofmann, and A. Ludwig. 2003. The hyperpolarization-activated channel HCN4 is required for the generation of pacemaker action potentials in the embryonic heart. *Proc. Natl. Acad. Sci. USA.* 100:15235–15240.

Sturm, K., and P.P.L. Tam. 1993. Isolation and culture of whole postimplantation embryos and germ layer derivatives. *Methods Enzymol.* 225:164–190.

Takeshima, H., S. Komazaki, K. Hirose, M. Nishi, T. Noda, and M. Lino. 1998. Embryonic lethality and abnormal cardiac myocytes in mice lacking ryanodine receptor type 2. *EMBO J.* 17:3309–3316.

Weissgerber, P., W. Bloch, B. Held, L. Kastner, P. Lipp, K. Chien, V. Flockerzi, and M. Freichel. 2005. Embryonic heart failure after disruption of the $Ca^{2+}$ channel subunit beta(2) gene (Ca-v beta(2)) leads to defects in vascular remodeling. *Naunyn Schmiedebergs Arch. Pharmacol.* 371:R55.

Viatchenko-Karpinski, S., B.K. Fleischmann, Q. Liu, H. Sauer, O. Gryshchenko, G.J. Ji, and J. Hescheler. 1999. Intracellular $Ca^{2+}$ oscillations drive spontaneous contractions in cardiomyocytes during early development. *Proc. Natl. Acad. Sci. USA.* 96:8259–8264.

Yang, Z., W. Shen, J.N. Rottman, J.P. Wikswo, and K.T. Murray. 2005. Rapid stimulation causes electrical remodeling in cultured atrial myocytes. *J. Mol. Cell. Cardiol.* 38:299–308.

Yasui, K., W. Liu, T. Opthof, K. Kada, J.K. Lee, K. Kamiya, and I. Kodama. 2001. $I_f$ current and spontaneous activity in mouse embryonic ventricular myocytes. *Circ. Res.* 88:536–542.

Zimmermann, W.H., K. Schneiderbanger, P. Schubert, M. Didie, F. Munzel, J.F. Heubach, S. Kostin, W.L. Neuhuber, and T. Eschenhagen. 2002. Tissue engineering of a differentiated cardiac muscle construct. *Circ. Res.* 90:223–230.